

Article

How Micelles Influence the Optical Limiting Properties of Zinc Porphyrins and J-Aggregates for Picosecond Pulse Trains

Quan Miao ^{1,*}, Erping Sun ¹ and Yan Xu ^{1,2}

¹ College of Electronic and Information Engineering, Shandong University of Science and Technology, Qingdao 266590, China

² College of Electrical Engineering and Automation, Shandong University of Science and Technology, Qingdao 266590, China

* Correspondence: qmiao2014@sdust.edu.cn

Abstract: In this work, we studied nonlinear dynamics and optical limiting (OL) effects of pulse trains in zinc porphyrins meso-tetrakis methylpyridiniumyl (Zn^{2+} TMPyP) and meso-tetrakis sulfonatophenyl (Zn^{2+} TPPS) and porphyrin J-aggregates. The environments of zinc porphyrins were selected as aqueous solutions and micelles of sodium dodecyl sulfate (SDS) and cetyltrimethyl ammonium bromide (CTAB). Our numerical results show that both Zn^{2+} TMPyP and Zn^{2+} TPPS are good optical limiters in all solutions. Zn^{2+} TPPS in aqueous solutions shows the best OL effect. Micelles of SDS and CTAB produced less OL effects than the aqueous solutions. The main reason lies in the first excited singlet state and intersystem crossing depending on the electronic structures in different environments.

Keywords: optical limiting; porphyrin; spectroscopy; pulse train; rate equation

MSC: 78A60



Citation: Miao, Q.; Sun, E.; Xu, Y. How Micelles Influence the Optical Limiting Properties of Zinc Porphyrins and J-Aggregates for Picosecond Pulse Trains. *Axioms* **2023**, *12*, 23. <https://doi.org/10.3390/axioms12010023>

Academic Editors: Irina Papkova and Tatyana Yakovleva

Received: 17 November 2022

Revised: 17 December 2022

Accepted: 22 December 2022

Published: 25 December 2022



Copyright: © 2022 by the authors. Licensee MDPI, Basel, Switzerland. This article is an open access article distributed under the terms and conditions of the Creative Commons Attribution (CC BY) license (<https://creativecommons.org/licenses/by/4.0/>).

1. Introduction

Porphyrins have advantages as optical limiters and switching devices [1–7] basing on their extremely extended π -conjugated structures [8,9]. In addition, their competitive features such as intense transition dipole moments, broad absorption region in a visible spectrum, and large quantum yield for triplet state [10–13] made them be widely used in therapy and diagnostics [14–20].

Owing to the advantages of porphyrins' structure, many researchers tried to make some modifications to increase their molecular properties by adding different central metal ions or peripherally substitutes [11,21–25], putting them in different solvents [26–29], binding to some proteins [30–34] et al. Recently, zinc(II) meso-tetrakis methylpyridiniumyl (Zn^{2+} TMPyP), zinc(II) meso-tetrakis sulfonatophenyl (Zn^{2+} TPPS), their J-aggregates, and interactions with different micelles were the focus in a number of different studies [35–40]. Works about the interaction of micelles such as cetyltrimethylammonium bromide (CTAB) with porphyrins were studied [41–47]. Their results indicated that CTAB is beneficial to pharmaceutical practice and pharmacological system of supramolecular porphyrin-based assemblies.

In this work, we studied nonlinear dynamics and optical limiting (OL) of Zn^{2+} TMPyP, Zn^{2+} TPPS and their J-aggregates in the absence and in the presence of sodium dodecyl sulfate (SDS) and CTAB micelles. Porphyrins are classic reverse saturable absorption (RSA) molecules with larger excited state absorption cross sections than the ground state one. We considered the studied compounds as a five-state scheme. During propagation of long duration pulse trains, singlet–singlet or singlet–triplet absorption is the fundamental nonlinear absorption mechanism. Our numerical results reveal that Zn^{2+} TPPS has better OL effects than Zn^{2+} TMPyP, and the presence of micelles diminished the OL properties of porphyrins J-aggregates.

2. Method

The molecular structures of zinc(II) meso-tetrakis methylpyridiniumyl ($Zn^{2+}TMPyP$) and zinc(II) meso-tetrakis sulfonatophenyl ($Zn^{2+}TPPS$) were shown in Figure 1. A five-state scheme in Figure 2 was used instead of the structures. We considered the interactions of molecules with pulse trains, hence the two-step two-photon absorption can be $(S_0 \rightarrow S_1) \times (S_1 \rightarrow S_n)$ or $(S_0 \rightarrow S_1) \times (T_1 \rightarrow T_2)$.

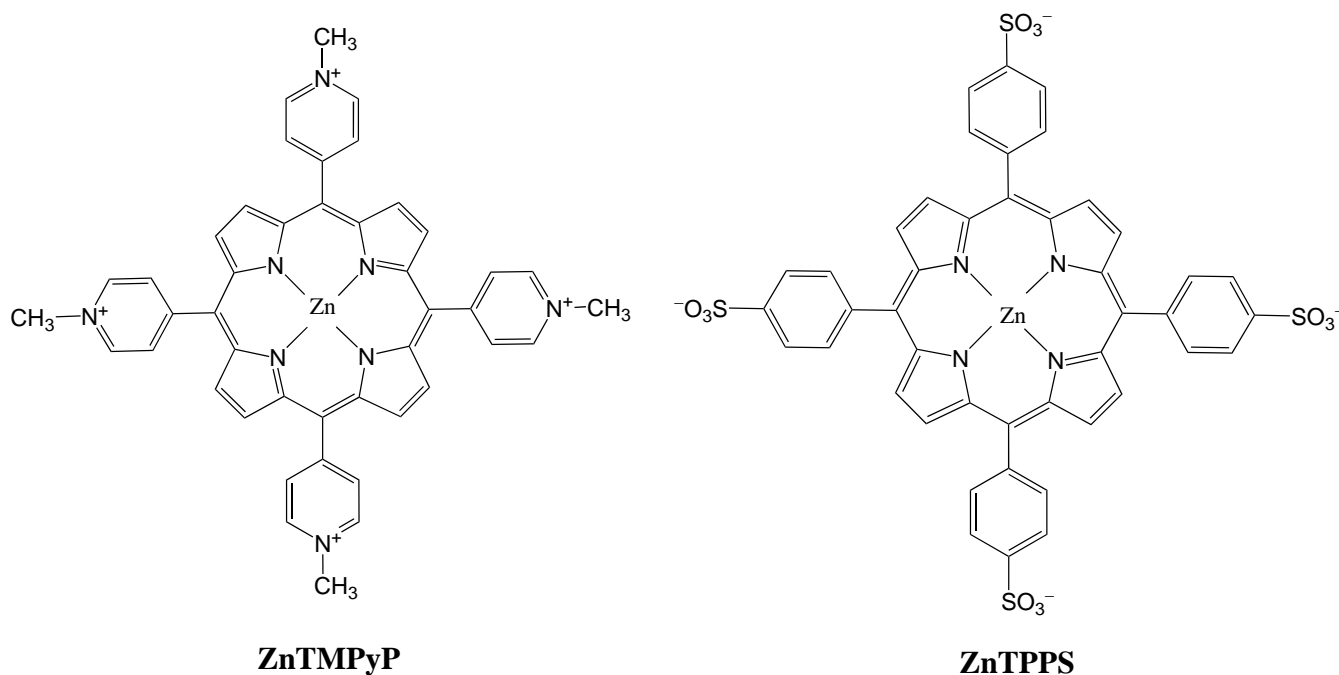


Figure 1. Structures of zinc(II) meso-tetrakis methylpyridiniumyl ($Zn^{2+}TMPyP$) and zinc(II) meso-tetrakis sulfonatophenyl ($Zn^{2+}TPPS$) [35,36].

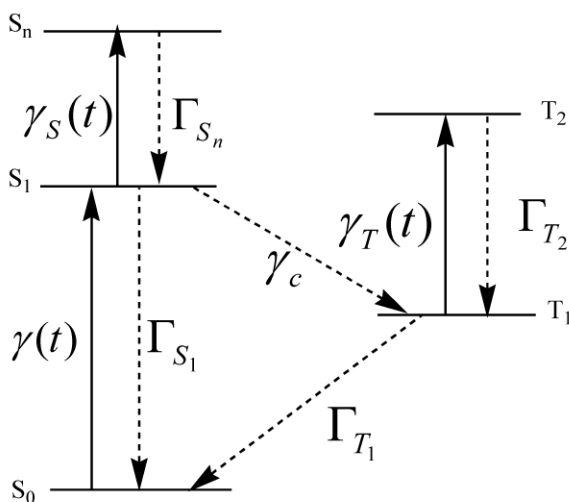


Figure 2. The Jablonski diagram of a five-level model.

The pulse train consists of a series of subpulses,

$$I(t) = \sum_{n=0} I_n(t), \quad n = 0, 1, \dots, n_{tot} - 1. \tag{1}$$

n and $n_{tot} = 20$ are the serial and total numbers of subpulses. Each subpulse was supposed to have the temporal shape of a rectangle [48,49],

$$I_n(r) = I_0 \exp \left[- \left(\frac{n\Delta - t_0}{\tau_e} \right)^2 \ln 2 \right] \exp \left[- \left(\frac{r}{r_0} \right)^2 \ln 2 \right]. \tag{2}$$

In this work, we considered picosecond pulse trains. Taking into account the data in the experiment [50], subpulse spacing is set as $\Delta = 13.2$ ns, and the duration for each subpulse is $\tau = 70$ ps. In addition, $r_0 = 2$ mm is the beam width of each initial subpulse. $t_0 = [(n_{tot} - 1)\Delta + \tau]/2$, $\tau_e = 10\Delta/3$.

The paraxial equation of time t and distance z for each subpulse is expressed as [48]

$$\left(\frac{\partial}{\partial z} - \frac{1}{c} \frac{\partial}{\partial t} \right) I_n(t) = -N \sum_{j>i} \sigma_{ij} (\rho_i - \rho_j) I_n(t). \tag{3}$$

$N = 2.9 \times 10^{23}/m^3$ is the concentration of molecules used in the experiment [50]. c is the speed of light in vacuum. Subscripts i and j were used to distinguish different states; then, σ_{ij} represents one-photon absorption cross section from low to high state $i \rightarrow j$. All state populations ρ can be calculated by the dynamical rate equations [51],

$$\begin{aligned} \frac{\partial}{\partial t} \rho_{S_0} &= -\gamma(t)(\rho_{S_0} - \rho_{S_1}) + \Gamma_{S_1} \rho_{S_1} + \Gamma_{T_1} \rho_{T_1}, \\ \left(\frac{\partial}{\partial t} + \Gamma_{S_1} + \gamma_c \right) \rho_{S_1} &= \Gamma_{S_n} \rho_{S_n} - \gamma_S(t)(\rho_{S_1} - \rho_{S_n}) + \gamma(t)(\rho_{S_0} - \rho_{S_1}), \\ \left(\frac{\partial}{\partial t} + \Gamma_{S_n} \right) \rho_{S_n} &= \gamma_S(t)(\rho_{S_1} - \rho_{S_n}), \\ \left(\frac{\partial}{\partial t} + \Gamma_{T_2} \right) \rho_{T_2} &= \gamma_T(t)(\rho_{T_1} - \rho_{T_2}), \quad \sum_k \rho_k = 1. \end{aligned} \tag{4}$$

Γ denotes the decay rate of the excited state's population and γ marks the opposite pump rate from low to high state. γ_c is the population transition rate of intersystem crossing (ISC) $S_1 \rightarrow T_1$, and $\gamma(t)$, $\gamma_S(t)$, $\gamma_T(t)$ are for the transitions $S_0 \rightarrow S_1$, $S_1 \rightarrow S_n$, $T_1 \rightarrow T_2$, respectively. Population pump rate γ is well known to relate to the corresponding cross section σ ,

$$\gamma_{ij}(t) = \frac{\sigma_{ij} I(t)}{\hbar \omega}. \tag{5}$$

ω is incident frequency of pulse trains and wave length is set as $\lambda = 2\pi c/\omega = 532$ nm in our calculations.

The transmittance of total energy for pulse trains was also calculated to estimate the OL effect,

$$\mathcal{T}(L) = \frac{J(z_0 + L)}{J(z_0)}. \tag{6}$$

The entrance and propagation distance of pulse trains is set as $z_0 = 0$ and L . Total energy $J(z)$ is the integral of instantaneous intensity $I(t, r, z)$ as follows:

$$J(z) = 2\pi \int_0^R \int_0^\infty I(t, r, z) r dr dt. \tag{7}$$

3. Results and Discussion

In our calculations, useful photophysical parameters of ZnTMPyP and ZnTPPS in aqueous solutions and their porphyrin J-aggregates with micelles of SDS and CTAB were collected in Table 1 from the experiment [50]. τ_{S_n} is set as 100 fs for ZnTMPyP and ZnTMPyP+SDS, and 1.3 ps for ZnTPPS and ZnTPPS+CTAB, respectively [50]. In addition,

concentrations for all compounds are set as $2.9 \times 10^{23} /\text{m}^3$ in consistent with the experiment [50]. Unfortunately, it did not give the lifetime of state T_1 in experiment [50]. We set τ_{T_1} for all compounds as 1.0×10^{-3} s according to another two experiments [26,30].

Table 1. Photophysical parameters of ZnTMPyP and ZnTPPS in aqueous solutions and their porphyrin J-aggregates with micelles of SDS and CTAB at $\lambda = 532$ nm [50]. $\gamma_c = 1/\tau_{isc}$, $\Gamma = 1/\tau$.

Compounds	τ_{S_1} (ns)	τ_{isc} (ns)	$\sigma_{S_0S_1}$ (m^2) $\times 10^{-21}$	$\sigma_{S_1S_n}$ (m^2) $\times 10^{-21}$	$\sigma_{T_1T_2}$ (m^2) $\times 10^{-21}$
ZnTMPyP	1.3	2.0	1.5	6.1	4.9
ZnTMPyP+SDS	1.4	1.5	1.4	4.0	2.4
ZnTPPS	1.8	2.2	1.7	4.3	7.0
ZnTPPS+CTAB	1.7	3.2	1.5	4.0	2.2

Firstly, we studied the energy transmittance $\mathcal{T}(L)$ depending on peak intensity of incident pulse trains in Figure 3 at distances $L = 0.5$ mm and $L = 1.0$ mm for all compounds. ZnTMPyP and ZnTPPS in aqueous solutions show lower transmittances than their J-aggregates with SDS and CTAB. For weak intensities, this difference is small. While the peak intensity increases higher than $I_0 = 1.0 \times 10^{12}$ W/m², the gap becomes obvious. In addition, we can notice that ZnTPPS in aqueous solutions has better OL behaviors than ZnTMPyP. At longer distance $L = 1.0$ mm, the overall trend is almost the same, but energy transmittances of all compounds decrease more rapidly, which is caused by more molecules taking part in the absorption.

In Figure 4, we plotted the dependences of the energy transmittance $\mathcal{T}(L)$ on distance L for all compounds with peak intensity $I_0 = 1.0 \times 10^{13}$ W/m². ZnTMPyP and ZnTPPS with SDS and CTAB have the very approximate curves, while ZnTMPyP and ZnTPPS in aqueous solutions could reach rather low values $\mathcal{T}(L) = 0.19$ and $\mathcal{T}(L) = 0.12$ at $L = 2$ mm, respectively.

Dynamical populations on five states were calculated, and we found two states S_0 and T_1 occupied almost all populations. In Figure 5, we plotted dynamical populations ρ_{S_0} and ρ_{T_1} at $L = 0$ with $I_0 = 1.0 \times 10^{12}$ W/m². For all compounds, the populations on state S_0 were transferred to T_1 mostly. We marked the 100% population transfer times, and ZnTPPS in aqueous solutions has the earliest time 105.6ns among all four compounds. ZnTMPyP with SDS has an earlier time than ZnTMPyP in aqueous solutions. Generally, τ_{S_1} and τ_{isc} are decisive parameters during population transferring in Table 1. Populations pumping on T_1 early ended up being instrumental in the one-photon absorption $T_1 \rightarrow T_2$, resulting in strong two-photon absorption.

Effective population transfer times τ_{ST} during absorption process $S_0 \rightarrow T_1$ [48] were studied and plotted in Figure 6. We could notice that τ_{ST} for all compounds are quite similar with weak intensities in two wing parts. In the middle part with high intensity, they are different apparently and ZnTPPS has the fastest transfer time τ_{ST} . Fast τ_{ST} would promote the residing of populations on state T_1 , which is mainly determined by the overall effect of τ_{S_1} and τ_{isc} in Table 1. Consequently, ZnTPPS in aqueous solutions has early and fast population transferring time and exhibits the best OL behaviors in Figures 3 and 4.

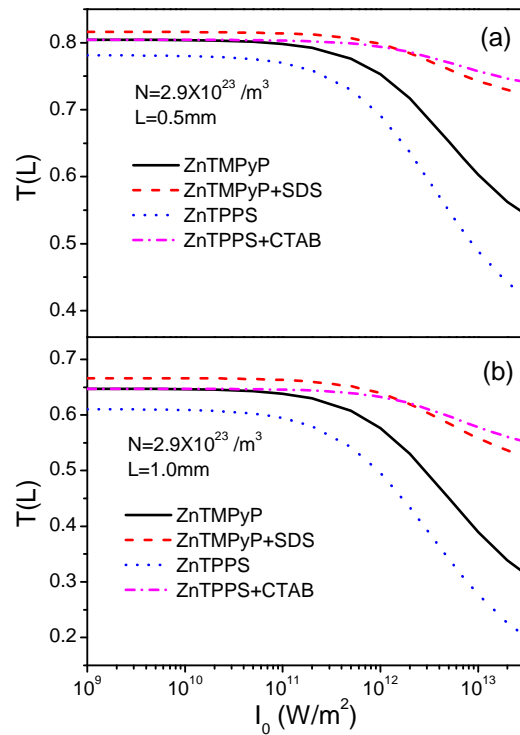


Figure 3. Energy transmittance $\mathcal{T}(L)$ (Equation (6)) as a function of the peak intensity of incident laser I_0 at (a) $L = 0.5$ mm and (b) $L = 1.0$ mm for ZnTMPyP and ZnTPPS in aqueous solutions and their porphyrin J-aggregates with micelles of SDS and CTAB. $N = 2.9 \times 10^{23} / m^3$.

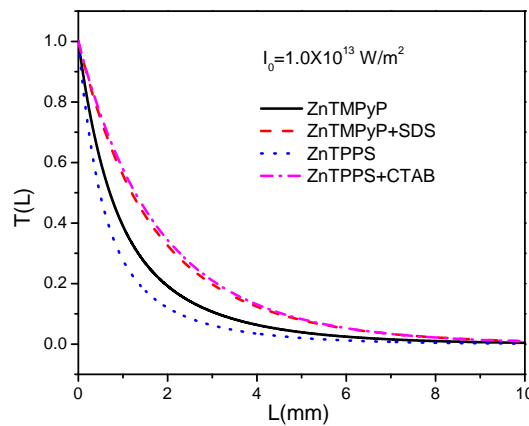


Figure 4. Energy transmittance $\mathcal{T}(L)$ (Equation (6)) as a function of the propagation distance L with $I_0 = 1.0 \times 10^{13} W/m^2$ for ZnTMPyP and ZnTPPS in aqueous solutions and their porphyrin J-aggregates with micelles of SDS and CTAB. $N = 2.9 \times 10^{23} / m^3$.

Taking ZnTPPS as an example, we studied the output intensities after OL absorption at $L = 1.0$ mm for different concentrations $N = 2.9 \times 10^{23} / m^3$, $N = 2.9 \times 10^{24} / m^3$ in Figure 7. At $r = 0$ in Figure 7a, we could see that the output intensity decreases 2~3 orders of magnitude with big concentration $N = 2.9 \times 10^{24} / m^3$, and the peak intensity occurs earlier than the cause with small concentration. Comparing the two-dimensional pictures Figure 7b,c, we could notice that the shape of output intensity becomes asymmetric with big concentration. This is because the front part is mainly the two-step absorption ($S_0 \rightarrow S_1$) \times ($T_1 \rightarrow T_2$), while the latter part is dominated by the one-photon absorption $T_1 \rightarrow T_2$ depending on population ρ_{T_1} . The different absorption mechanisms lead to the asymmetric phenomenon. Big concentration means more molecules taking part in the nonlinear absorption and therefore the asymmetry becomes more explicit.

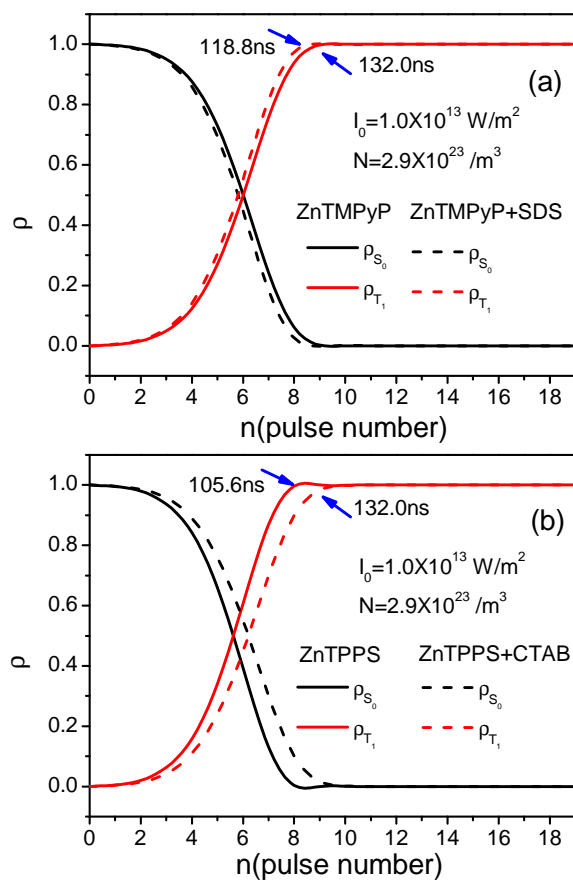


Figure 5. Population dynamics ρ_{S_0} and ρ_{T_1} at $L = 0$ for ZnTMPyP and ZnTPPS in aqueous solutions and their porphyrin J-aggregates with micelles of SDS and CTAB. (a) ZnTMPyP in aqueous solutions and in micelles of SDS. (b) ZnTPPS in aqueous solutions and in micelles of CTAB. $I_0 = 1.0 \times 10^{13} \text{ W/m}^2$, $N = 2.9 \times 10^{23} /\text{m}^3$.

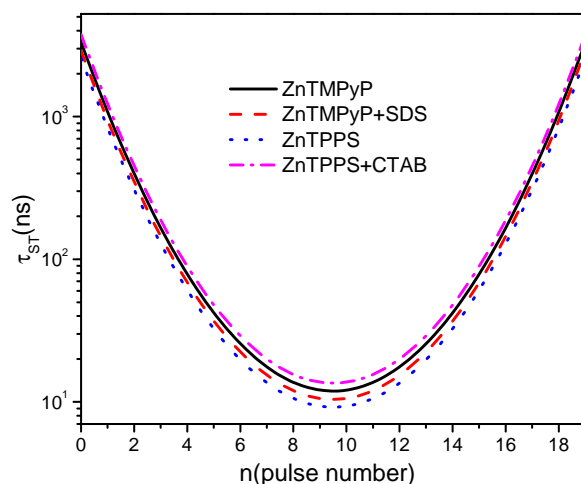


Figure 6. The effective population transfer time τ_{ST} at $L = 0$ and $r = 0$ for ZnTMPyP and ZnTPPS in aqueous solutions and their porphyrin J-aggregates with micelles of SDS and CTAB. $I_0 = 1.0 \times 10^{13} \text{ W/m}^2$, $N = 2.9 \times 10^{23} /\text{m}^3$.

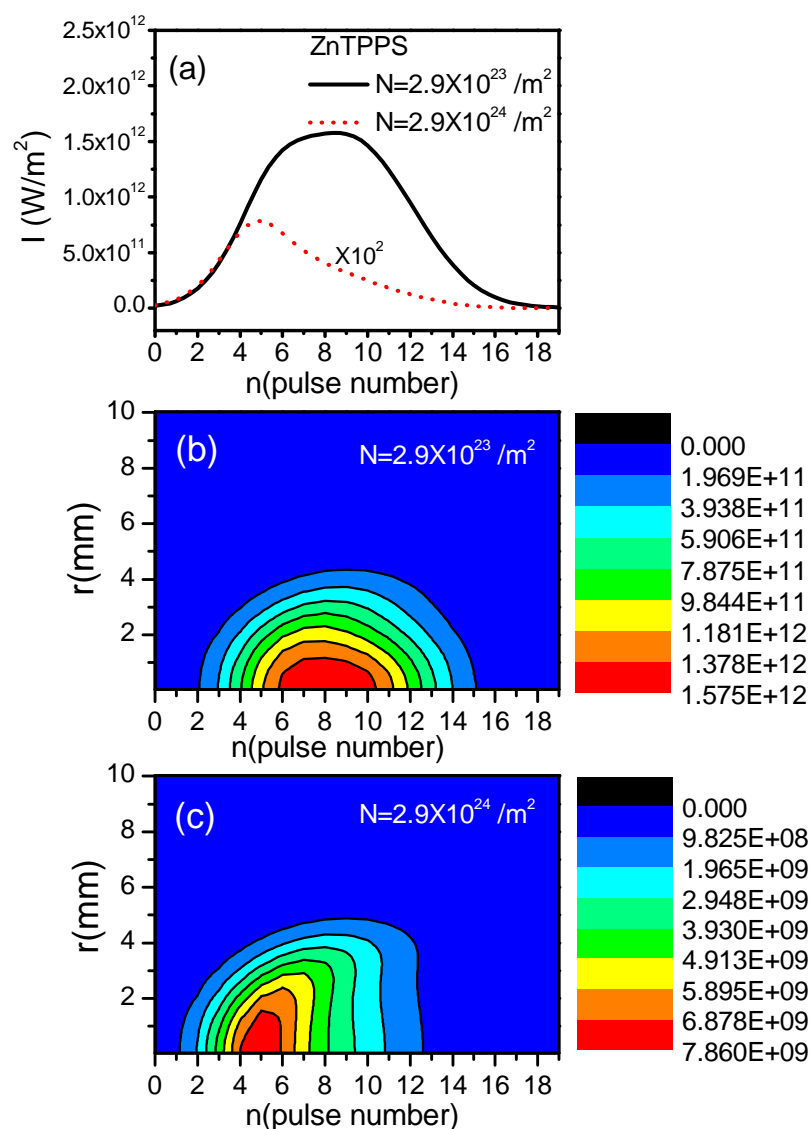


Figure 7. The laser intensities after absorbing at $L = 1.0$ mm with $I_0 = 1.0 \times 10^{13}$ W/m² for ZnTPPS in aqueous solutions. (a) the intensities at $r = 0$; (b) two-dimensional picture with $N = 2.9 \times 10^{23}$ /m³; (c) two-dimensional picture with $N = 2.9 \times 10^{24}$ /m³.

4. Conclusions

Dynamical absorption processes of picosecond pulse trains in ZnTMPyP and ZnTPPS in aqueous solutions and their porphyrin J-aggregates with micelles of SDS and CTAB were studied in this work. Interacting with picosecond pulse trains, the studied materials were simplified as a five-level model. We used the Crank–Nicholson numerical method to solve rate equations and the two-dimensional paraxial field. The OL process is mainly two-step absorption ($S_0 \rightarrow S_1$) \times ($T_1 \rightarrow T_2$). For weak intensities, there is mainly the linear absorption. However, for high intensities, the nonlinear two-step absorption is dominant, and the output intensities would be extremely asymmetric. All compounds are good optical limiters, and ZnTPPS in aqueous solutions shows the best OL properties mainly due to the combined effect of photophysical parameters τ_{S_1} and τ_{isc} . In general, micelles of SDS and CTAB would weaken the OL effects of ZnTMPyP and ZnTPPS. Increasing concentration is one effective method to enhance the OL effect.

Author Contributions: Conceptualization, Q.M.; Data curation, Q.M.; Funding acquisition, Q.M.; Project administration, Y.X.; Visualization, E.S.; Writing—original draft, Q.M. All authors have read and agreed to the published version of the manuscript.

Funding: This research was funded by the Youth Expert program of Taishan scholars of Shandong Province, China and Natural Science Foundation of Shandong Province, China Grant Nos. ZR2022MA085 and ZR2019MA020.

Data Availability Statement: The data that support the findings of this research are available from the corresponding author upon reasonable request.

Acknowledgments: Financial support from the Youth Expert program of Taishan scholars of Shandong Province, China and Natural Science Foundation of Shandong Province, China (Grant Nos. ZR2022MA085 and ZR2019MA020) is gratefully acknowledged.

Conflicts of Interest: The authors declare no conflict of interest. The funders had no role in the design of the study; in the collection, analyses, or interpretation of data; in the writing of the manuscript; or in the decision to publish the results.

References

1. Singh, C.P.; Bindra, K.S.; Jain, B.; Oak, S.M. All-optical switching characteristics of metalloporphyrins. *Opt. Commun.* **2005**, *245*, 407. [[CrossRef](#)]
2. Liu, M.O.; Tai, C.H.; Hu, A.T.; Wei, T.H. Reverse saturable absorption of lanthanide bisphthalocyanines and their application for optical switches. *J. Organomet. Chem.* **2004**, *689*, 2138. [[CrossRef](#)]
3. Dini, D.; Calvete, M.J.F.; Hanack, M. Nonlinear optical materials for the smart filtering of optical radiation. *Chem. Rev.* **2016**, *116*, 13043. [[CrossRef](#)] [[PubMed](#)]
4. Calvete, M.; Yang, G.Y.; Hanack, M. Porphyrins and phthalocyanines as materials for optical limiting. *Synth. Met.* **2004**, *141*, 231. [[CrossRef](#)]
5. Thanopoulos, I.; Paspalakis, E.; Yannopoulos, V. Optical switching of electric charge transfer pathways in porphyrin: A light-controlled nanoscale current router. *Nanotechnology* **2008**, *19*, 445202. [[CrossRef](#)]
6. Barbosa, N.M.; Oliveira, S.L.; Misoguti, L.; Mendonca, C.R.; Goncalves, P.J.; Borissevitch, I.E.; Dinelli, L.R.; Romualdo, L.L.; Batista, A.A.; Zilio, S.C. Singlet excited state absorption of porphyrin molecules for pico- and femtosecond optical limiting application. *J. Appl. Phys.* **2006**, *99*, 123103. [[CrossRef](#)]
7. Xu, Y.F.; Liu, Z.B.; Zhang, X.L.; Wang, Y.; Tian, J.G.; Huang, Y.; Ma, Y.F.; Zhang, X.Y.; Chen, Y.S. A Graphene Hybrid Material Covalently Functionalized with Porphyrin: Synthesis and Optical Limiting Property. *Adv. Mater.* **2009**, *21*, 1275. [[CrossRef](#)]
8. Senge, M.O.; Fazekas, M.; Notaras, E.G.A.; Blau, W.J.; Zawadzka, M.; Locos, O.B.; Mhuircheartaigh, E.M.N. Nonlinear Optical Properties of Porphyrins. *Adv. Mater.* **2007**, *19*, 2737. [[CrossRef](#)]
9. de la Torre, G.; Vaquez, P.; Agullo-Lopez, F.; Torres, T. Role of Structural Factors in the Nonlinear Optical Properties of Phthalocyanines and Related Compounds. *Chem. Rev.* **2004**, *104*, 3723. [[CrossRef](#)]
10. Horiuchi, H.; Kameya, T.; Hosaka, M.; Yoshimura, K.; Kyushin, S.; Matsumoto, H.; Okutsu, T.; Takeuchi, T.; Hiratsuka, H. Silylation enhancement of photodynamic activity of tetraphenylporphyrin derivative. *J. Photochem. Photobiol.* **2001**, *A 221*, 98. [[CrossRef](#)]
11. Kubat, P.; Mosinger, J. Photophysical properties of metal complexes of meso-tetrakis(4-sulphonatophenyl)porphyrin. *J. Photochem. Photobiol. A Chem.* **1996**, *96*, 93. [[CrossRef](#)]
12. Monteiro, C.J.P.; Serpa, C.; Pereira, M.M.; Azenha, M.E.; Burrows, H.D.; Arnaut, L.G.; Tapia, M.J.; Sarakha, M.; Navaratnam, S. A comparative study of water soluble 5,10,15,20-tetrakis(2,6-dichloro-3-sulfophenyl)porphyrin and its metal complexes as efficient sensitizers for photodegradation of phenols. *Photochem. Photobiol. Sci.* **2005**, *4*, 617. [[CrossRef](#)]
13. Dudkowiak, A.; Teslak, E.; Habdas, J. Photophysical studies of tetraolyporphyrin photosensitizers for potential medical applications. *J. Mol. Struct.* **2006**, 792–793, 93. [[CrossRef](#)]
14. Bonnett, R. Photosensitizers of the porphyrin and phthalocyanine series for photodynamic therapy. *Chem. Soc. Rev.* **1995**, *24*, 19. [[CrossRef](#)]
15. Ochsner, M. Photophysical and photobiological processes in the photodynamic therapy of tumours. *J. Photochem. Photobiol.* **1997**, *39*, 1. [[CrossRef](#)]
16. Jasuja, R.; Jameson, D.M.; Nishijo, C.K.; Larsen, R.W. Singlet Excited State Dynamics of Tetrakis(4-N-methylpyridyl)porphine Associated with DNA Nucleotides. *J. Phys. Chem. B* **1997**, *101*, 1444. [[CrossRef](#)]
17. Uno, T.; Hamasaki, K.; Tanigawa, M.; Shimabayashi, S. Binding of meso-Tetrakis(N-methylpyridinium-4-yl)porphyrin to Double Helical RNA and DNA-RNA Hybrids. *Inorg. Chem.* **1997**, *36*, 1676. [[CrossRef](#)]
18. Josefsen, L.B.; Boyle, R.W. Unique diagnostic and therapeutic roles of porphyrins and phthalocyanines in photodynamic therapy, imaging and theranostics. *Theranostics* **2012**, *9*, 916. [[CrossRef](#)]
19. Taratula, O.; Schumann, C.; Naleway, M.A.; Pang, A.J.; Chon, K.J.; Taratula, O. A multifunctional theranostic platform based on phthalocyanine-loaded dendrimer for image-guided drug delivery and photodynamic therapy. *Mol. Pharm.* **2013**, *10*, 3946. [[CrossRef](#)]

20. Pucelik, B.; Paczynski, R.; Dubin, G.; Pereira, M.M.; Arnaut, L.G.; Dabrowski, J.M. Properties of halogenated and sulfonated porphyrins relevant for the selection of photosensitizers in anticancer and antimicrobial therapies. *PLoS ONE* **2017**, *12*, e0185984. [[CrossRef](#)]
21. Goncalves, P.J.; De Boni, L.; Barbosa, N.M.; Rodrigues, J.J., Jr.; Zilio, S.C.; Borissevitch, I.E. Effect of protonation on the photophysical properties of meso-tetra(sulfonatophenyl) porphyrin. *Chem. Phys. Lett.* **2005**, *407*, 236. [[CrossRef](#)]
22. Goncalves, P.J.; Borissevitch, I.E.; Zilio, S.C. Effect of protonation on the singlet–singlet excited-state absorption of meso-tetrakis(p-sulphonatophenyl) porphyrin. *Chem. Phys. Lett.* **2009**, *469*, 270. [[CrossRef](#)]
23. Sampaio, R.N.; Gomes, W.R.; Araujo, D.M.S.; Machado, A.E.H.; Silva, R.A.; Marletta, A.; Borissevitch, I.E.; Ito, A.S.; Dinelli, L.R.; Batista, A.A.; et al. Investigation of Ground- and Excited-State Photophysical Properties of 5,10,15,20-Tetra(4-pyridyl)-21H,23H-porphyrin with Ruthenium Outlying Complexes. *J. Phys. Chem. A* **2012**, *116*, 18. [[CrossRef](#)] [[PubMed](#)]
24. Goncalves, P.J.; De Boni, L.; Borissevitch, I.E.; Zilio, S.C. Excited State Dynamics of meso-Tetra(sulphonatophenyl) Metalloporphyrins. *J. Phys. Chem. A* **2008**, *112*, 6522. [[CrossRef](#)] [[PubMed](#)]
25. Pavani, C.; Uchoa, A.F.; Oliveira, C.S.; Yamamoto, Y.; Baptista, M.S. Effect of zinc insertion and hydrophobicity on the membrane interactions and PDT activity of porphyrin photosensitizers. *Photochem. Photobiol. Sci.* **2009**, *8*, 233. [[CrossRef](#)]
26. Goncalves, P.J.; Franzen, P.L.; Correa, D.S.; Almeida, L.M.; Takara, M.; Ito, A.S.; Zilio, S.C.; Borissevitch, I.E. Effects of environment on the photophysical characteristics of mesotetrakis methylpyridiniumyl porphyrin (TMPyP). *Spectrochim. Acta Part A* **2011**, *79*, 1532. [[CrossRef](#)]
27. Reddi, E.; Ceccon, M.; Valduga, G.; Jori, G.; Bommer, J.C.; Elisei, F.; Latterini, L.; Mazzucato, U. Photophysical Properties and Antibacterial Activity of Meso-substituted Cationic Porphyrins. *Photochem. Photobiol.* **2002**, *75*, 462. [[CrossRef](#)]
28. Snyder, J.W.; Lambert, J.D.C.; Ogilby, P.R. 5,10,15,20-Tetrakis(N-Methyl-4-Pyridyl)-21 H,23H-Porphine (TMPyP) as a Sensitizer for Singlet Oxygen Imaging in Cells: Characterizing the Irradiation-dependent Behavior of TMPyP in a Single Cell. *Photochem. Photobiol.* **2006**, *82*, 177. [[CrossRef](#)]
29. Jimenez-Banzo, A.; Sagrista, M.L.; Mora, M.; Nonell, S. Kinetics of singlet oxygen photosensitization in human skin fibroblasts. *Free Radic. Biol. Med.* **2008**, *44*, 1926. [[CrossRef](#)]
30. Goncalves, P.J.; Bezerra, F.C.; Almeida, L.M.; Alonso, L.; Souza, G.R.L.; Alonso, A.; Zilio, S.C.; Borissevitch, I.E. Effects of bovine serum albumin (BSA) on the excited-state properties of meso-tetrakis(sulfonatophenyl) porphyrin (TPPS4). *Eur. Biophys. J.* **2019**, *48*, 721. [[CrossRef](#)]
31. Borissevitch, I.E.; Tominaga, T.T.; Schmitt, C.C. Photophysical studies on the interaction of two water soluble porphyrins with bovine serum albumin. Effects upon the porphyrin triplet state characteristics. *J. Photochem. Photobiol. A* **1998**, *114*, 201. [[CrossRef](#)]
32. Andrade, S.M.; Costa, S.M.B. Spectroscopic studies on the interaction of a water soluble porphyrin and two drug carrier proteins. *Biophys. J.* **2002**, *82*, 1607. [[CrossRef](#)]
33. Dubbelman, T.M.A.R. Porphyrin-protein interaction. In *Photosensitisation*; Moreno, G., Pottier, R.H., Truscott, T.G., Eds.; NATO ASI Series (Series H: Cell Biology); Springer: Berlin, Germany, 1988; Volume 15.
34. Morgan, W.T.; Smith, A.; Koskelo, P. The interaction of human serum albumin and hemopexin with porphyrins. *BBA Protein Struct.* **1980**, *624*, 271. [[CrossRef](#)]
35. Kadish, K.M.; Maiya, G.B.; Araullo, C.; Guillard, R. Micellar effects on the aggregation of tetraanionic porphyrins. Spectroscopic characterization of free-base meso-tetrakis(4-sulfonatophenyl)porphyrin, (TPPS)H₂, and (TPPS)M (M = zinc(II), copper(II), and vanadyl) in aqueous micellar media. *Inorg. Chem.* **1989**, *28*, 2725. [[CrossRef](#)]
36. Kadish, K.M.; Maiya, B.G.; Araullo-McAdams, C. Spectroscopic characterization of meso-tetrakis(1-methylpyridinium-4-yl)porphyrins, [(TMPyP)H₂]⁴⁺ and [(TMPyP)M]⁴⁺, in aqueous micellar media, where M = VO₂⁺, Cu(II), and Zn(II). *J. Phys. Chem.* **1991**, *95*, 427. [[CrossRef](#)]
37. Gandini, S.C.; Yushmanov, V.E.; Tabak, M. Interaction of Fe(III)- and Zn(II)-tetra(4-sulfonatophenyl) porphyrins with ionic and nonionic surfactants: Aggregation and binding. *J. Inorg. Biochem.* **2001**, *85*, 263. [[CrossRef](#)]
38. Wang, X.; Zhao, L.; Ma, R.; An Y.; Shi, Y. Stability enhancement of ZnTPPS in acidic aqueous solutions by polymeric micelles. *Chem. Commun.* **2010**, *46*, 6560. [[CrossRef](#)]
39. Szymtkowski, J.; Brunet, S.M.K.; Tripathy, U.; O'Brien, J.A.; Paige, M.P.; Steer, R.P. Photophysics and halide quenching of Soret-excited ZnTPPS⁴⁻ in aqueous media. *Chem. Phys. Lett.* **2011**, *501*, 278. [[CrossRef](#)]
40. Lebold, T.P.; Yeow, K.L.; Steer, R.P. Fluorescence quenching of the S₁ and S₂ states of zinc meso-tetrakis(4-sulfonatophenyl)porphyrin by halide ions. *Photochem. Photobiol. Sci.* **2004**, *3*, 160. [[CrossRef](#)]
41. Zhao, B.; Li, Y.; Zhao, Y.; Ma, Y.; Li, F.; Han, H.; Wang, N.; Wang, X. A sensing platform based on zinc-porphyrin derivative in hexadecyl trimethyl ammonium bromide (CTAB) microemulsion for highly sensitive detection of theophylline. *Spectrochim. Acta Part A: Mol. Biomol. Spectrosc.* **2022**, *281*, 121592. [[CrossRef](#)]
42. Mamardashvili, G.M.; Kaigorodova, E.Y.; Lebedev, I.S.; Khodov, I.A.; Mamardashvili, N.Z. Supramolecular assembly of hydrophilic Co(III)-porphyrin with bidentate ligands in aqueous buffer media. *Inorganica Chim. Acta* **2022**, *538*, 120972. [[CrossRef](#)]
43. Wang, X.; Zhang, S.; Zhao, B. Determination of ultra trace amounts of metronidazole by 3-phenyl-N-[4-(10,15,20-triphenylporphyrin-5-yl)-phenyl]-acrylamide as the fluorescence spectral probe in CTAB microemulsion. *Spectrochim. Acta Part A Mol. Biomol. Spectrosc.* **2020**, *227*, 117699. [[CrossRef](#)]

44. Mamardashvili, G.M.; Kaigorodova, E.Y.; Khodov, I.A.; Sheblykin, I.; Nugzar, Z.; Mamardashvili, N.Z.; Koifman, O.I. Micelles encapsulated Co(III)-tetra(4-sulfophenyl)porphyrin in aqueous CTAB solutions: Micelle formation, imidazole binding and redox Co(III)/Co(II) processes. *J. Mol. Liq.* **2019**, *293*, 111471. [[CrossRef](#)]
45. Guo, L. Side-chain-controlled H- and J-aggregation of amphiphilic porphyrins in CTAB micelles. *J. Colloid Interface Sci.* **2008**, *322*, 281–286. [[CrossRef](#)]
46. Goncalves, P.J.; Aggarwal, L.P.F.; Marquezin, C.A.; Ito, A.S.; Boni, L.D.; Neto, N.M.B.; Rodrigues, J.J., Jr.; Zilio, S.C.; Borissevitch, I.E. Effects of interaction with CTAB micelles on photophysical characteristics of meso-tetrakis(sulfonatophenyl) porphyrin. *J. Photochem. Photobiol. A Chem.* **2006**, *181*, 378–384. [[CrossRef](#)]
47. Amao, Y.; Tomonou, Y.; Okura, I. Highly efficient photochemical hydrogen production system using zinc porphyrin and hydrogenase in CTAB micellar system. *Sol. Energy Mater. Sol. Cells* **2003**, *79*, 103–111. [[CrossRef](#)]
48. Sun, Y.P.; Gavriluk, S.; Liu, J.C.; Wang, C.K.; Ågren, H.; Gel'mukhanov, F. Optical limiting and pulse reshaping of picosecond pulse trains by fullerene C60. *J. Electron. Spectrosc. Relat. Phenom.* **2009**, *174*, 125. [[CrossRef](#)]
49. Gel'mukhanov, F.; Ågren, H. Resonant X-ray Raman scattering. *Phys. Rep.* **1999**, *312*, 87. [[CrossRef](#)]
50. Goncalves, P.J.; Correa, D.S.; Franzen, P.L.; De Boni, L.; Almeida, L.M.; Mendonca, C.R.; Borissevitch, I.E.; Zilio, S.C. Effect of interaction with micelles on the excited-state optical properties of zinc porphyrins and J-aggregates formation. *Spectrochim. Acta Part A Mol. Biomol. Spectrosc.* **2013**, *112*, 309. [[CrossRef](#)]
51. Gavriluk, S.; Liu, J.C.; Kamada, K.; Ågren, H.; Gel'mukhanov, F. Optical limiting for microsecond pulses. *J. Chem. Phys.* **2009**, *130*, 054114. [[CrossRef](#)]

Disclaimer/Publisher's Note: The statements, opinions and data contained in all publications are solely those of the individual author(s) and contributor(s) and not of MDPI and/or the editor(s). MDPI and/or the editor(s) disclaim responsibility for any injury to people or property resulting from any ideas, methods, instructions or products referred to in the content.